Design and Analysis of Tow-Steered Composite Shells Using Fiber Placement

K. Chauncey Wu
NASA Langley Research Center
Hampton, Virginia

ABSTRACT

In this study, a sub-scale advanced composite shell design is evaluated to determine its potential for use on a future aircraft fuselage. Two composite shells with the same nominal 8-ply $[\pm 45/\pm\Theta]_S$ layup are evaluated, where Θ indicates a tow-steered ply. To build this shell, a fiber placement machine would be used to steer unidirectional prepreg tows as they are placed around the circumference of a 17-inch diameter right circular cylinder. The fiber orientation angle varies continuously from 10 degrees (with respect to the shell axis of revolution) at the crown, to 45 degrees on the side, and back to 10 degrees on the keel. All 24 tows are placed at each point on every fiber path in one structure designated as the shell with overlaps. The resulting pattern of tow overlaps causes the laminate thickness to vary between 8 and 16 plies. The second shell without tow overlaps uses the capability of the fiber placement machine to cut and add tows at any point along the fiber paths to fabricate a shell with a nearly uniform 8-ply laminate thickness. Issues encountered during the design and analysis of these shells are presented and discussed. Static stiffness and buckling loads of shells with tow-steered layups are compared with the performance of a baseline quasi-isotropic shell using both finite element analyses and classical strength of materials theory.

INTRODUCTION

Computer-numerically-controlled fiber placement machines [1] were first introduced to the commercial market in the late 1980s. These highly automated systems are enabling technology for the fabrication of advanced composite structures, defined here as ones in which the fiber orientation angle is allowed to vary continuously throughout a structure within a given ply [2]. Thus, the local fiber orientation angle in each ply of an advanced composite structure may become

---

K. Chauncey Wu: Aerospace Engineer, Structural Mechanics and Concepts Branch, RTD. NASA Langley Research Center, Mail Stop 190, Hampton, VA 23681. k.c.wu@nasa.gov

a design variable. These additional design variables allow extensive tailoring of the structural response to the applied loads, resulting in improved performance and reduced weight over a conventional composite structure where the fiber orientation angle is held straight and parallel throughout any given ply. The laminate thickness may also be varied in both conventional and advanced composite structures.

While extensive research has been done on flat panels with tow-steered layups [3, 4], relatively little effort has been invested in the design and analysis of advanced composite shells. In this study, a sub-scale shell concept is evaluated to determine its potential for use on a future aircraft fuselage. Details such as doors and windows are not included. Two composite shells, a design with tow overlaps and one without overlaps are evaluated. Both shells have the same nominal 8-ply $[\pm 45/\pm\Theta]_S$ layup, where Θ indicates a ply with steered tows.

Since the dominant operational loading of an aircraft fuselage is bending about the span-wise axis from aerodynamic and inertial forces, a common structural analog for a fuselage is an I-beam. The general layup of these shells thus aims to orient the composite fibers along the fuselage length on the crown and keel in Figure 1a (corresponding to the upper and lower flanges of the I-beam) for high extensional stiffness to resist the flight bending loads. In addition, the shell sides (corresponding to the shear web of the I-beam) provide high shear stiffness to resist the relative deflection of the crown and keel.

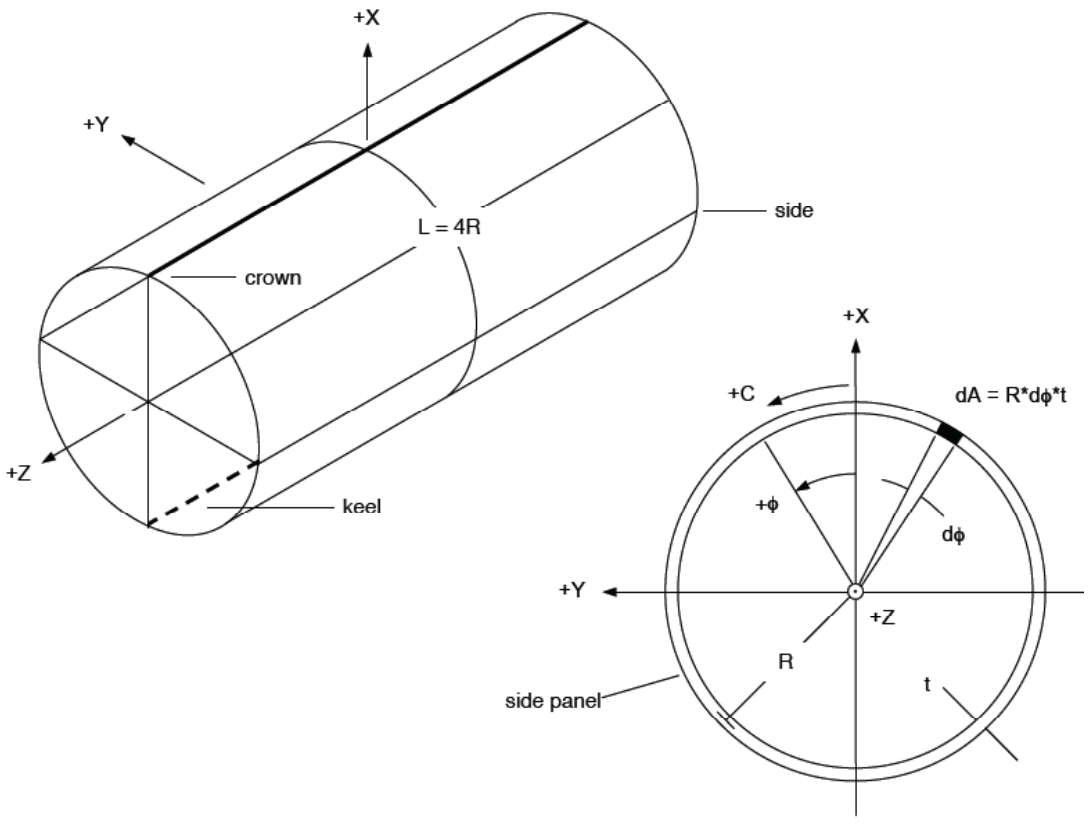

Figure 1a. Tow-steered shell schematic.

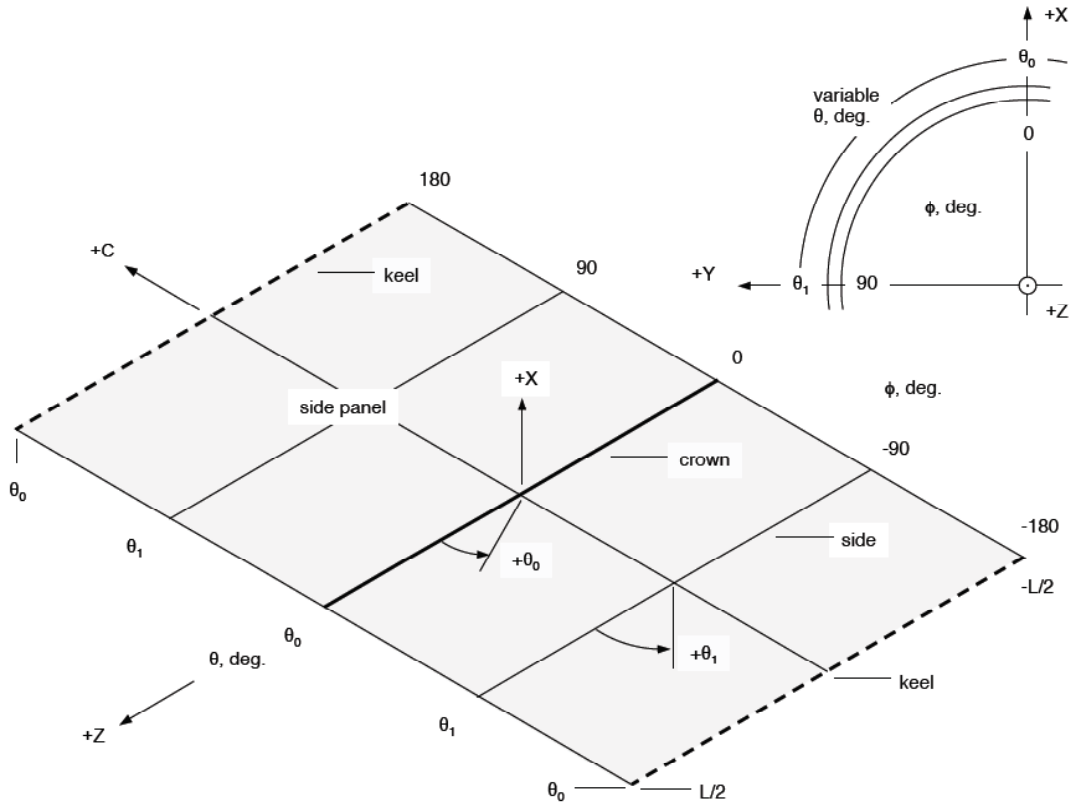

Figure 1b. Tow-steered shell planform.

To manufacture this advanced composite shell, a fiber placement machine would be used to steer composite tows as they are placed around the circumference of a right circular cylinder (radius R = 8.5 inches) used as the mandrel. The fiber orientation angle θ, measured with respect to the shell axis of revolution (see Figure 1b), varies continuously from 10 degrees at the crown (where the shell circumferential angle ϕ is equal to zero), to 45 degrees on the sides (ϕ = 90 degrees), and back to 10 degrees on the keel (ϕ = 180 degrees).

The associated continuous tow paths, or courses, resemble helical paths around the shell surface, and permit continuous load transfer from crown to side to keel. The number of tows that can be placed during each course is determined by the capabilities of an individual fiber placement machine, and ranges from a single tow to a typical maximum of 24 to 32 tows, with a typical tow width of 0.125 inches. The tow band width is the product of the number of tows placed during a course and the individual tow width.

Various issues encountered during the design and analysis of these shells are presented and discussed. Structural performance estimates for these tow-steered shells are made using both finite element analyses and classical strength of materials theory, and are then compared with corresponding results for a baseline quasi-isotropic shell. Additional issues relevant to manufacturing these shells are also noted.

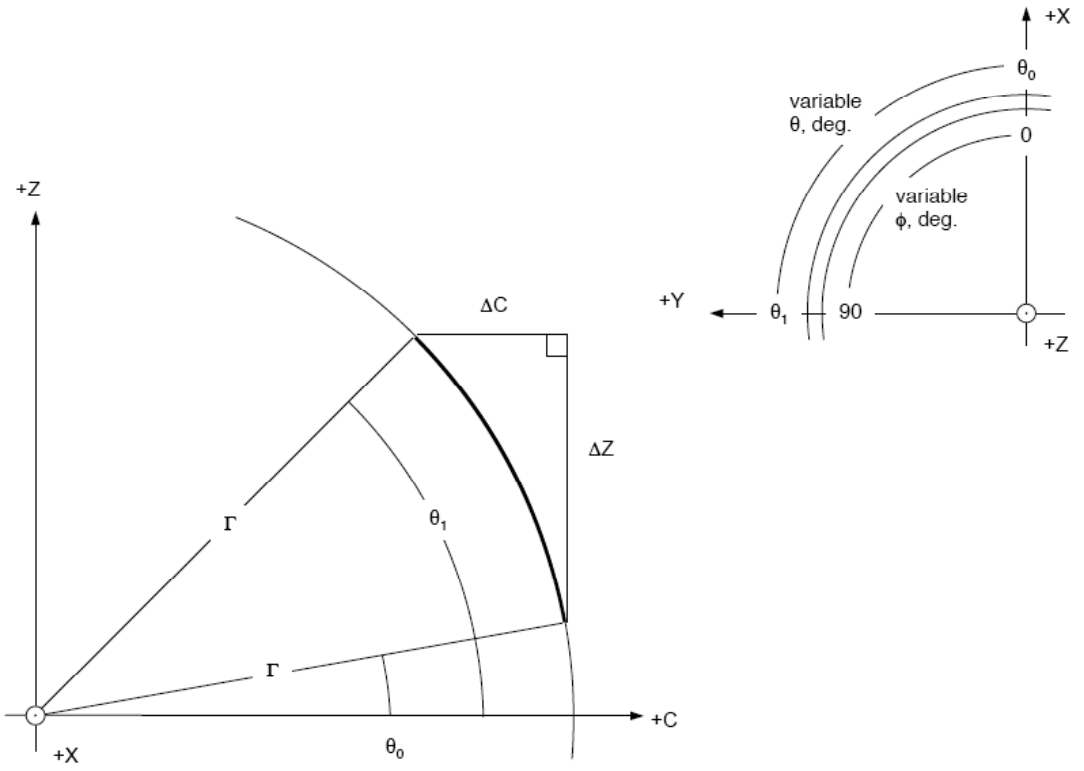

Figure 2. Circular-arc tow path with constant radius.

TOW- STEERED COURSE DESIGN

In this section, the curvilinear paths followed by the fiber placement machine during fabrication of these shells are defined and described. Tow paths for the ±45 degree plies are not discussed here, since they are considered to be well within the current state of the art in fiber placement. A circular arc with constant radius Γ (see Figure 2) is first defined where the fiber orientation angle θ varies from $\theta_0 = 10$ degrees at the beginning of the arc, to $\theta_1 = 45$ degrees at the end. Since the dimension

$$\Delta C = \Gamma[\cos(\theta_0) - \cos(\theta_1)] \tag{1}$$

is equal to the one-fourth of the mandrel circumference, or 13.352 inches, this relationship is used to determine the reference tow path radius of curvature Γ = 48.080 inches.

The minimum circular arc radius that can be fabricated is determined by the capabilities of the fiber placement machine that will be used to build the shells. This minimum circular arc radius can be as large as 24 inches [5]. The circular arc is then translated in space so that the end with $\theta = \theta_0$ is located at the origin of the shell surface coordinate system. Finally, the circular arc is reflected about the circumferential and axial axes to form the complete reference tow path (see Figure 3), which is centered at the center of the shell planform. An identical copy of the

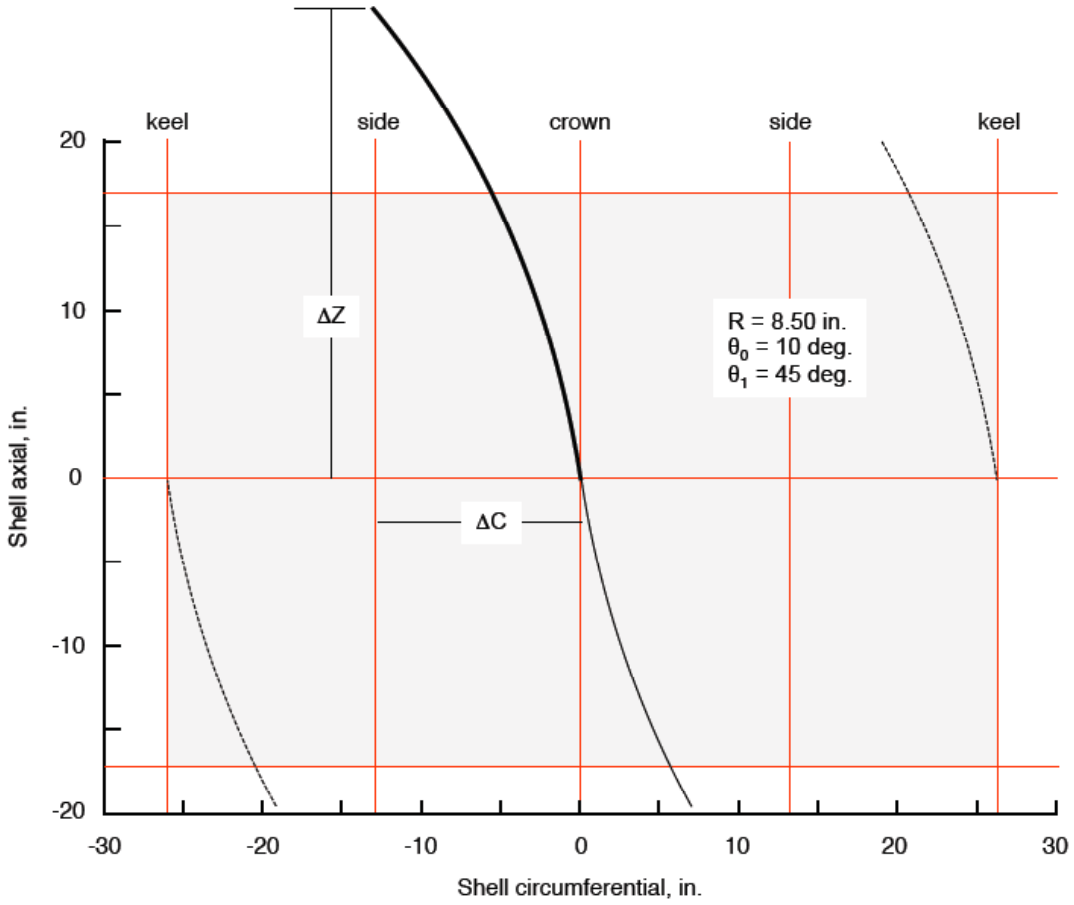

Figure 3. Complete reference tow path.

reference tow path is also centered at the middle of the shell keel line, and is shown as a dashed line in Figure 3.

After definition of the reference tow path, the shell surface is fully populated with identical copies of the reference tow path. These copies are created by translating the reference tow path in both the positive and negative shell axial directions. A close approximation to the magnitude of these axial shift increments is shown in Figure 4, and is computed as

$$SI = (\text{number of tows x tow width} + \varepsilon)/\sin(\theta_1), \quad (2)$$

where the step-over dimension ε is a small, constant increment selected to ensure that each course does not overlap previously placed, adjacent courses along the shell side. The product of the number of tows and the individual tow width is TBW, the tow band width shown in the figure.

The number of tows placed in each course and the step-over are then chosen so that the dimension

$$\Delta Z = \Gamma[\sin(\theta_1) - \sin(\theta_0)], \quad (3)$$

or 25.649 inches, divided by the axial shift increment in Equation 2 is either an

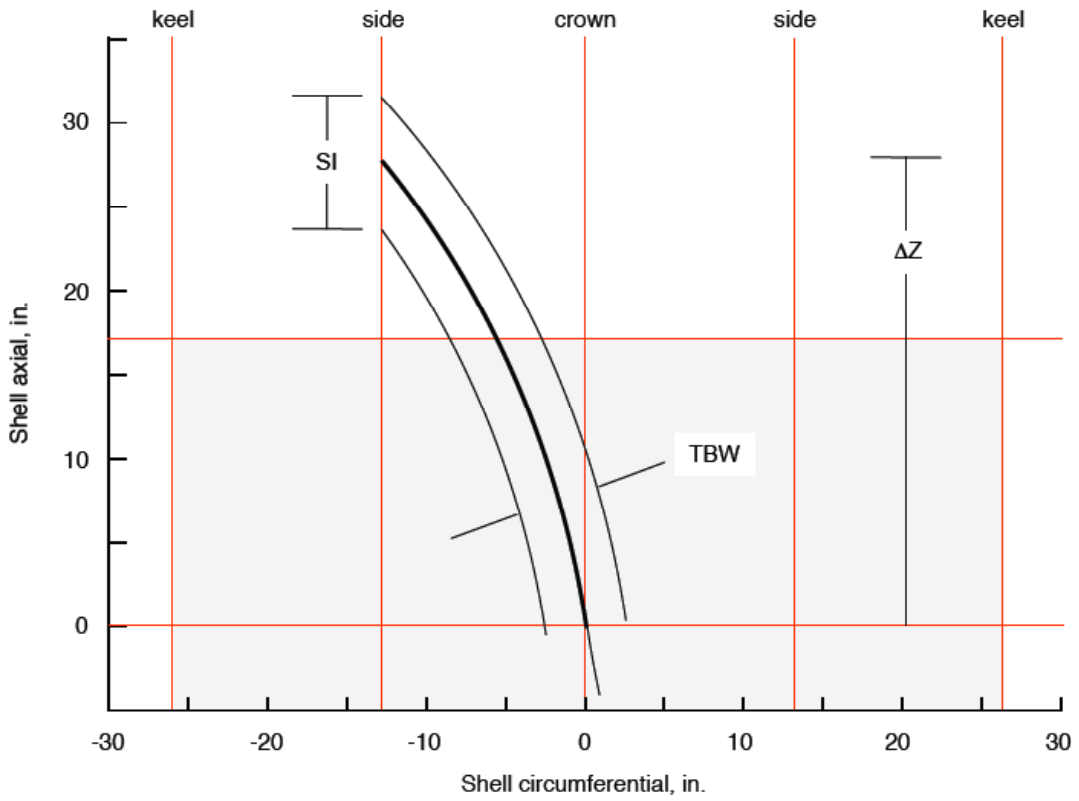

Figure 4. Shift increment definition.

integer or an integer divided by two. This course spacing ensures that successive courses will be adjacent along the shell sides as they are placed on the mandrel.

For the present tow-steered shell configuration, the fiber placement machine is assumed to be capable of placing a maximum of 24 tows per course. Table I shows the resulting number of courses necessary to cover the dimension ΔZ. These values are computed for placement of between 6 and 24 tows per course, with discrete step-overs varying from 0 to 0.040 inches. Many viable combinations are shown in the table. For example, acceptable solutions are placement of a total of 9 courses with 16 tows per course and a 0.015-inch step-over, or a total of 13 courses with 11 tows per course and a 0.020-inch step-over.

After further examination of the data in Table I, a solution having 6 courses with 24 tows per course and a 0.023-inch step-over (interpolated between the bolded numbers in the table) is selected. This configuration allows the largest number of tows to be placed during each course, thus minimizing the total time required to manufacture the shell. A total of 24 courses are needed to completely cover the mandrel surface. These course centerlines are shown in Figure 5, which is a planform view of the shell surface for the +Θ ply.

Since the mandrel diameter is assumed to be exactly 17 inches, placement of the inner ±45-degree plies will increase the diameter of the surface on which the subsequent tow-steered plies are placed. Using a nominal ply thickness of 0.00765 inches [2], the effective "mandrel" diameter for the first tow-steered ply is (17 in. + 4 plies x 0.00765 in./ply) = 17.031 inches.

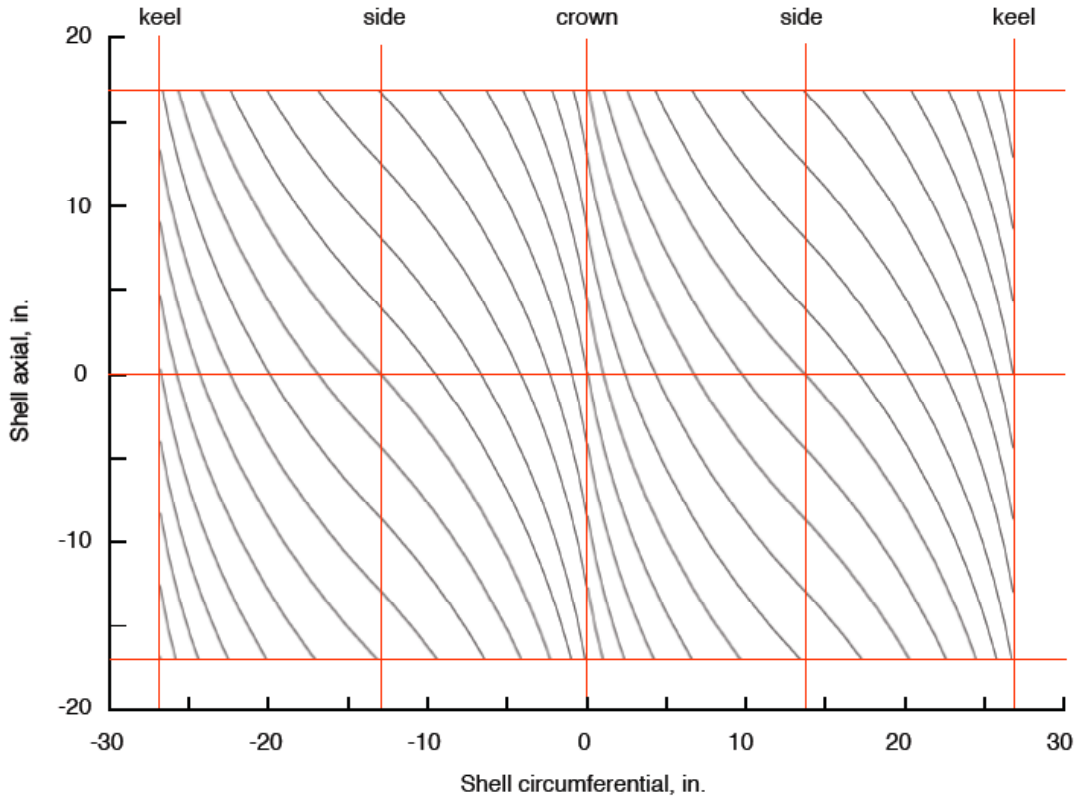

Figure 5. Shell planform with tow-steered course centerlines.

For fabrication of an actual tow-steered shell, this small variation in diameter for each ply must be factored into determination of the reference tow path radius of curvature and step-over for each ply, which would both vary slightly from the results presented above. However, since the number of tows placed during each tow-steered course and the number of courses will not change, these minor effects are neglected here to simplify the present discussion.

SHELL MANUFACTURING MODELS

Two composite shell configurations with the tow-steered layup are described here. Both shells have the same nominal 8-ply $[\pm 45/\pm\Theta]_S$ layup, where Θ indicates a ply with steered tows. For the first design, designated as the shell with tow overlaps, all 24 tows are placed at each point on each course. The ideal resulting pattern of tow overlaps for this shell is shown in Figure 6, with the laminate thickness varying from 8 to 16 plies in discrete steps. The second shell without tow overlaps uses the capability of the fiber placement machine to cut and add tows at any point along the fiber path to fabricate a shell with a nearly uniform 8-ply laminate thickness.

Manufacturing models of these tow-steered shells are then created using simulated course data based on the tow paths shown in Figure 5. Data for the tow-steered and straight-fiber ±45-degree plies are assembled in the proper order

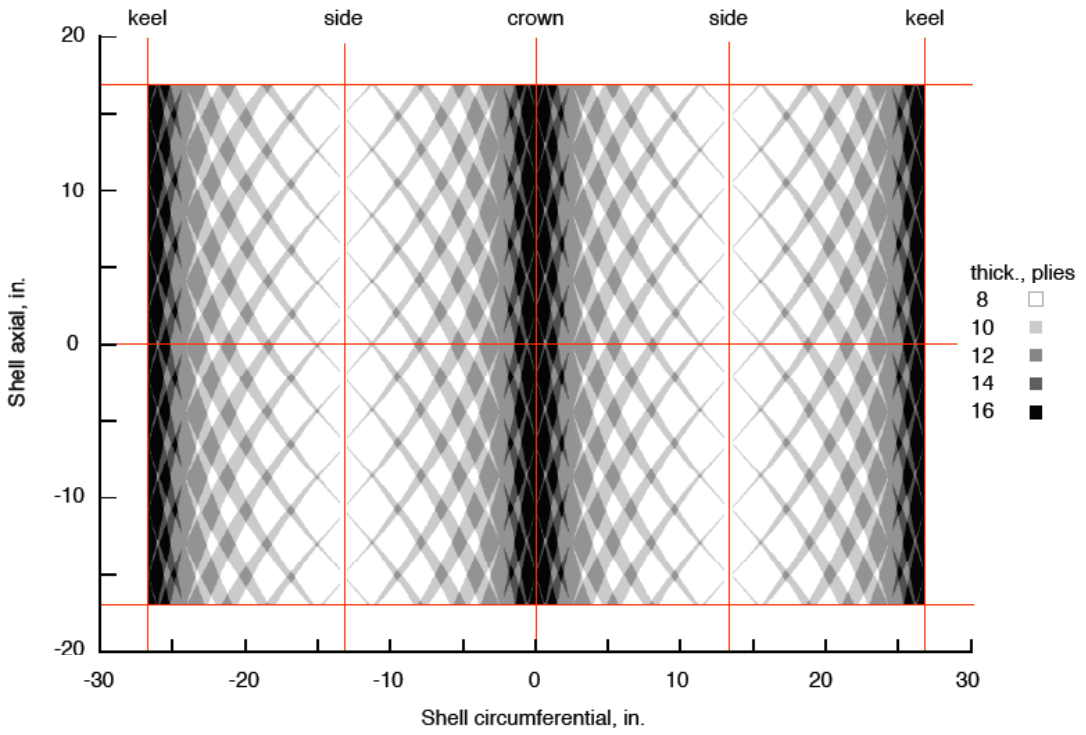

Figure 6. Ideal tow overlaps pattern of shell with overlaps.

and read into a computer program, which is then used to determine the laminate thickness and stacking sequence at an orthogonal grid of points (spaced at 0.207 x 0.133 inches in the circumferential and axial directions) over the shell surface.

The predicted laminate thicknesses for the shell with overlaps from this analysis range from 8 to 18 plies, and are shown as a contour plot in Figure 7. Qualitatively, the overlap features from the manufacturing model resemble the ideal pattern of overlaps in Figure 6, especially around the shell sides. However, the predicted overlaps pattern from the manufacturing model, computed on a relatively coarse grid, is less refined than the ideal pattern around the crown and keel lines.

The corresponding predicted fiber orientation angles for the first tow-steered ply (ply 3) of the shell with overlaps are shown as a contour plot in Figure 8. The fiber orientation angles vary from 10 degrees (dark gray) along the crown and keel lines, to 45 degrees (white) on the sides. There are also scattered locations across the shell surface, indicated as black dots, where the predicted fiber orientation angles are equal to –45 degrees. These points arise from overlapped tows in the ±45-degree plies previously placed on the mandrel.

Although both shells will have localized resin-rich regions and discontinuities in the load paths throughout their planform, these features arise for very different reasons. For the shell with overlaps, they occur where a placed tow is overlapped with previously placed tows, resulting in “bridging” of the fibers. However, for the shell without overlaps, these anomalies will occur wherever tows are cut (forming a tow drop there) or added, preventing the tow overlaps seen in Figures 6 and 7 while still placing the fibers on their desired curvilinear paths.

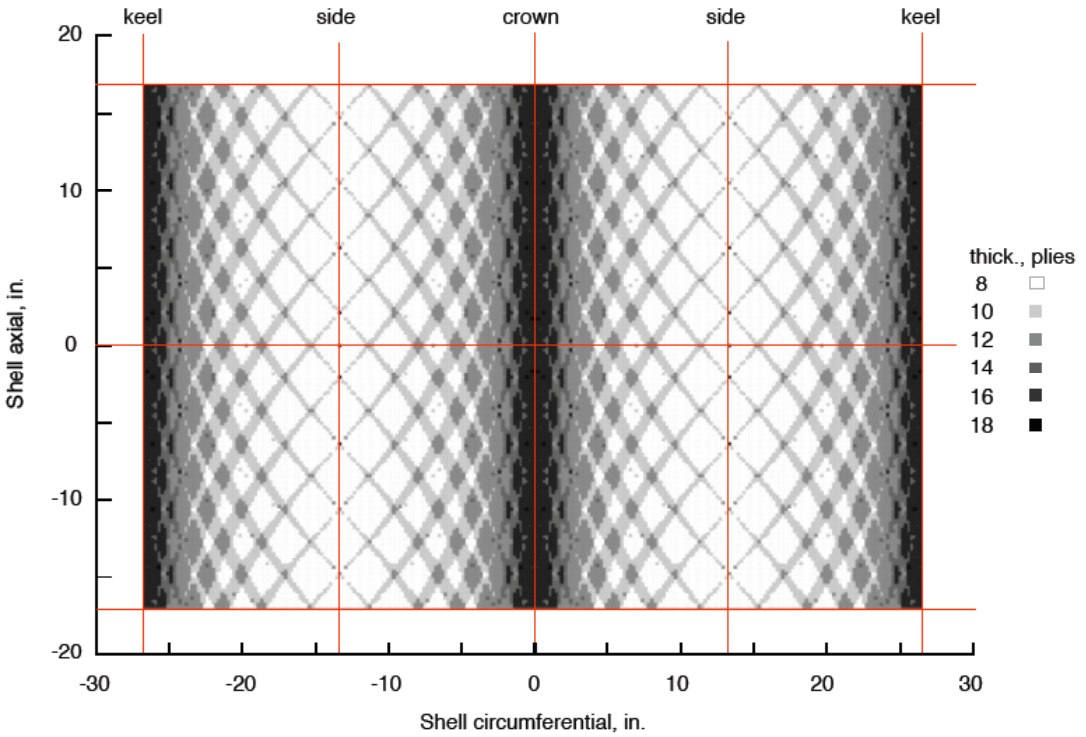

Figure 7. Shell with overlaps predicted laminate thicknesses.

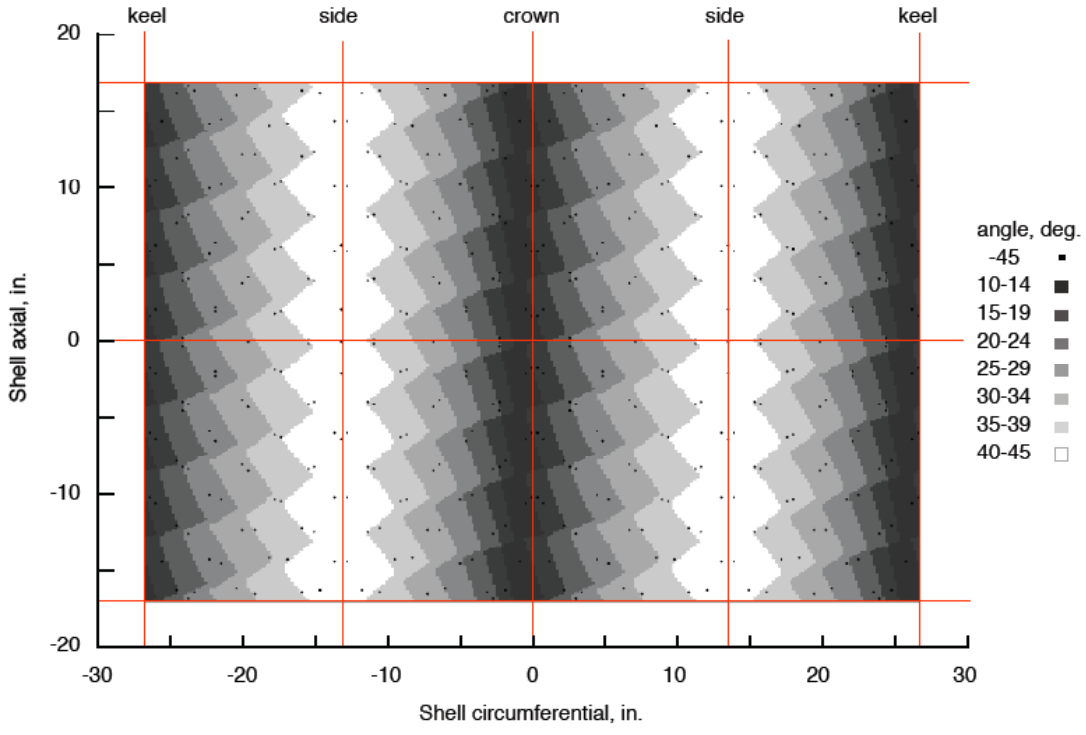

Figure 8. Shell with overlaps ply 3 predicted fiber angles.

For the shell without overlaps, the integer number of tows placed during each tow-steered course varies from a minimum of one tow to a maximum of 24 tows. The 2080 tow drops for ply 3 of the shell without overlaps are shown as black dots in Figure 9, which is a contour plot of the predicted fiber orientation angles for that tow-steered ply. Tow drop locations are coincident for the two tow-steered plies with the same orientation, and also where the lines of tow drops from the ±Θ plies intersect. For fabrication of thicker laminates, techniques such as non-integer shifting of the tow courses may be employed to prevent too many coincident tow drops. Tow drop locations for the –Θ plies nay be visualized by reflecting the tow drops shown in the figure about the shell crown line.

The predicted weights for the tow-steered shells with and without overlaps are computed using the data plotted in Figures 7 and 9. For the shell with overlaps, the laminate thicknesses in Figure 7 are used to determine an estimate of the cured shell weight. For each of the discrete laminate thicknesses between 8 and 18 plies, the number of points with that thickness is determined and multiplied by that laminate thickness value and the differential shell area of 0.207 x 0.133 inches around each location. These data are then added together and multiplied by the 0.00765-inch ply thickness and the nominal material density of 0.058 lb/in^3. This process results in a predicted weight of 8.38 lbs for the shell with overlaps.

The predicted weight for the shell without overlaps is computed by first subtracting the 2080 tow drops shown in Figure 9 from the 67077 total points for that ply. The resulting 64997 points in each of the four tow-steered plies are added to the 67077 points in each of the four ±45-degree plies. The 528296 total points are then multiplied by the product of the differential area, the ply thickness and the

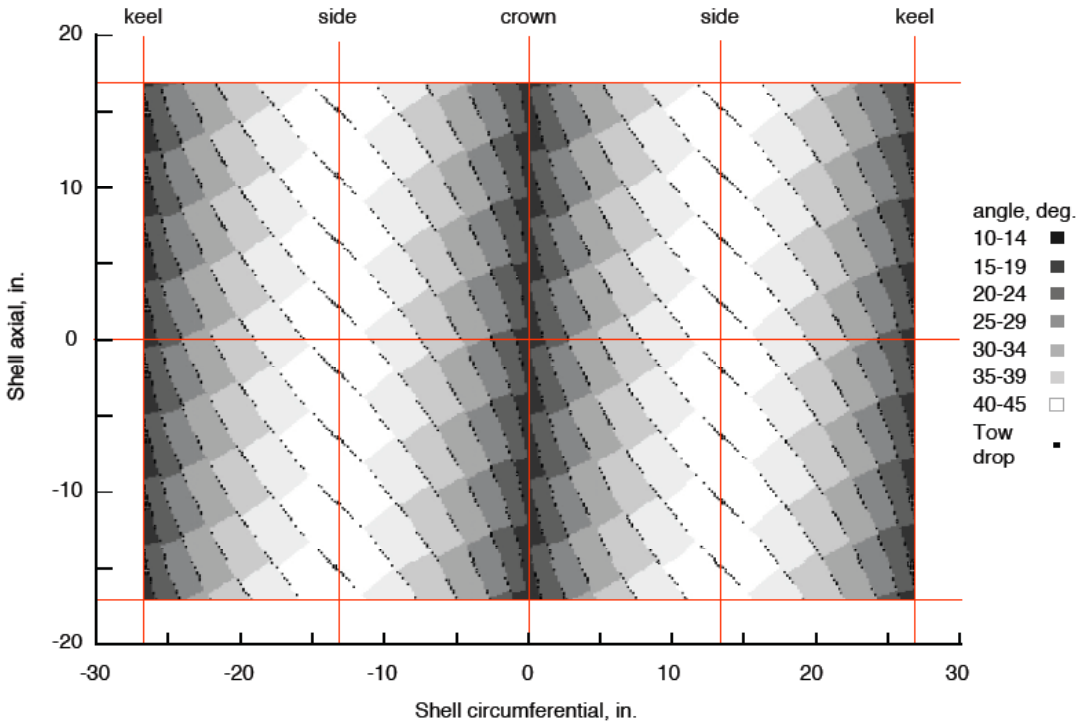

Figure 9. Shell without overlaps ply 3 predicted fiber angles and tow drops.

material density to get a predicted weight for the shell without overlaps of 6.45 lbs. Similarly, the predicted weight of the quasi-isotropic baseline shell is 6.56 lbs, with the 1.6 percent weight difference being due to the tow drops.

SHELL FINITE ELEMENT MODELS

For both shell finite element analysis models, a nodal mesh is defined that has 120 elements around the shell circumference and 68 elements along the shell length. The model has a total of 8160 elements, each 0.446 x 0.500 inches in the circumferential and axial directions, respectively. Boundary conditions for the model consist of fully clamped conditions imposed at one end of the 34-inch long right circular cylinder, with a closed ring of rigid beam elements defined at the opposite free end. Axial forces are applied to selected nodes on the free end of the shell, which then induce pure bending in the shell. Measured material properties [2] for an AS4/977-3 prepreg tow with a 0.00765-inch ply thickness are used here. These values are E_1 = 18.83 Mlb/in^2, E_2 = 1.34 Mlb/in^2, G_{12} = 0.74 Mlb/in^2 and ν_{12} = 0.36.

The shell with overlaps manufacturing model described in the previous section is used here to define the laminate thicknesses and fiber orientation angles for a finite element model of that shell. The nodal mesh described above is overlaid on the manufacturing model shown in Figure 7. Each finite element in this analysis model mesh encompasses about 9 data points from the manufacturing model.

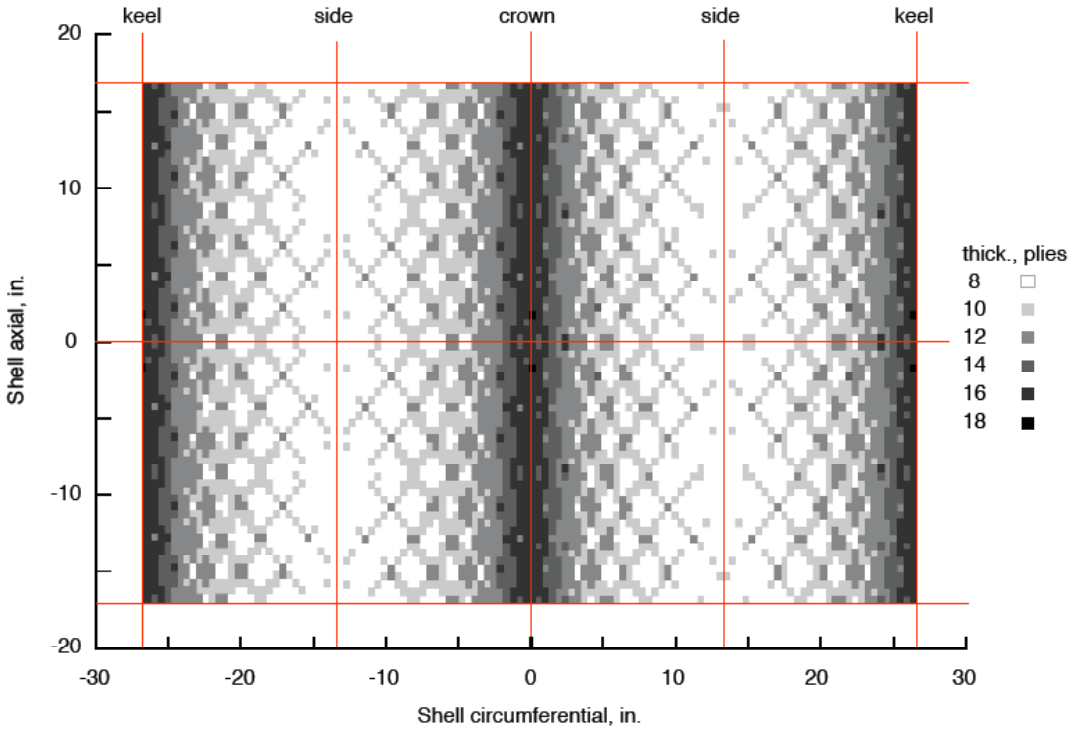

Figure 10. Shell with overlaps FE model discretized laminate thicknesses.

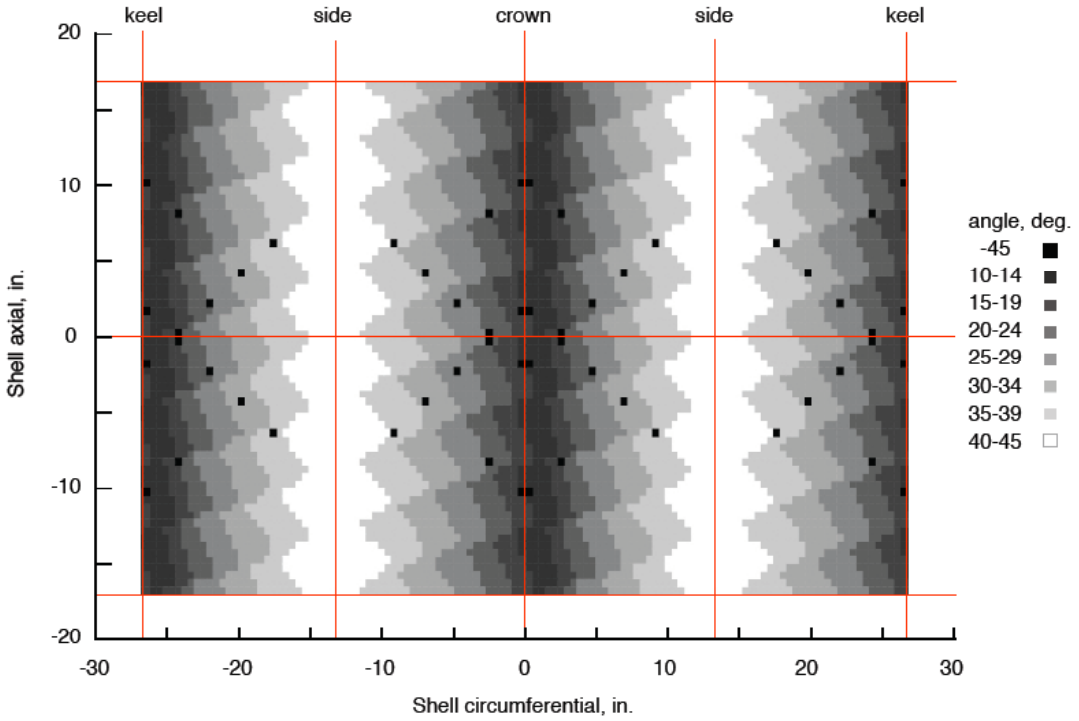

Figure 11. Shell with overlaps FE model ply 3 discretized fiber angles.

To assign shell properties to the finite elements, the centroid of a given finite element is first located. The laminate thickness and corresponding layup at the mesh location in the manufacturing model (see Figures 7 and 8) that is closest to the element centroid are then assigned to that finite element. This process is repeated until a unique laminate thickness and layup has been defined for each finite element in the analysis model.

The discretized laminate thicknesses for the finite element model of the shell with overlaps are shown in Figure 10. These thicknesses range from 8 to 18 plies, and resemble a coarser version of the predicted patterns in Figures 6 and 7. The fiber orientation angles for the first tow-steered ply of the shell with overlaps are shown in Figure 11. These angles range from 10 to 45 degrees over most of the planform, with –45 degrees angles in a limited number of elements.

For the shell without overlaps, the tow drops shown in Figure 9 are neglected when generating the finite element model. A closed-form relationship between the fiber orientation angle θ and the shell circumferential angle ϕ (measured in radians) is derived from the arc length ϕR and Equation 1 above. This equation is given as

$$\theta(\phi) = \cos^{-1}[\cos(\theta_0) - \phi R/\Gamma], \tag{4}$$

where R is the shell radius and Γ is the reference tow path radii of curvature as defined above.

Equation 4 is then used to compute the fiber orientation angle for axial groups of finite elements located at the same circumferential angle and running along the

entire shell length. The shell's two planes of symmetry are also used to reduce the number of unique element types that must be defined by a factor of 4. Since there are 120 finite elements distributed around the shell circumference, only 30 unique layups are needed for this model, with each element covering 3 degrees of arc.

SHELL STRUCTURAL ANALYSES

The structural models described above are then evaluated using the STAGS finite element analysis code [6] to predict the performance of the tow-steered shells under applied bending moments. Shell bending stiffnesses, as well as critical moments for linear bifurcation buckling, of the shells with and without overlaps are computed and compared with corresponding values for a quasi-isotropic $[\pm 45/0/90]_S$ shell.

When two axial forces are applied in opposite directions at the shell free end, a pure bending moment is generated. The effective bending stiffnesses EI of the shells are computed using two formulas derived from strength of materials [7] for a cantilevered prismatic beam under an end moment. These relationships are given as

$$EI = ML^2/(2\Delta_{end}) \tag{5}$$

and

$$EI = ML/\gamma_{end}, \tag{6}$$

where M is the applied bending moment, L is the shell length, and Δ_{end} and γ_{end} are the resulting deflection and rotation of the shell free end. The computed average of these effective stiffnesses for bending in both the X- and Y-axes are listed in Table II. The data presented are the averages of the individual bending stiffnesses computed using Equations 5 and 6, and differ by at most ±0.05 percent.

The bending stiffnesses for the shell with overlaps range from 67 percent greater than to 40 percent less than the 868.1 Mlb-in^2 bending stiffness of the quasi-isotropic shell. The additional material from the tow overlaps oriented along the shell crown and keel contributes greatly to the shell Y-bending stiffness when that material is loaded axially. Corresponding values for the shell without overlaps show a 10 to 50 percent reduction in bending stiffnesses over the baseline shell.

The applied bending moments are then used to compute linear bifurcation buckling moments for the tow-steered and baseline shells. These predicted buckling moments from the STAGS analyses are reported in Table II. Buckling moments for the shell with overlaps are from 40 percent greater than to 14 percent less than the 428.3 klb-in. moment for the quasi-isotropic shell. Buckling moments for the shell without overlaps range from 66 to 49 percent of the baseline value.

SHELLS WITH CROWN/KEEL PANELS

With the exception of Y-axis bending of the shell with overlaps, the tow-steered shells have lower structural performance when compared with the baseline quasi-

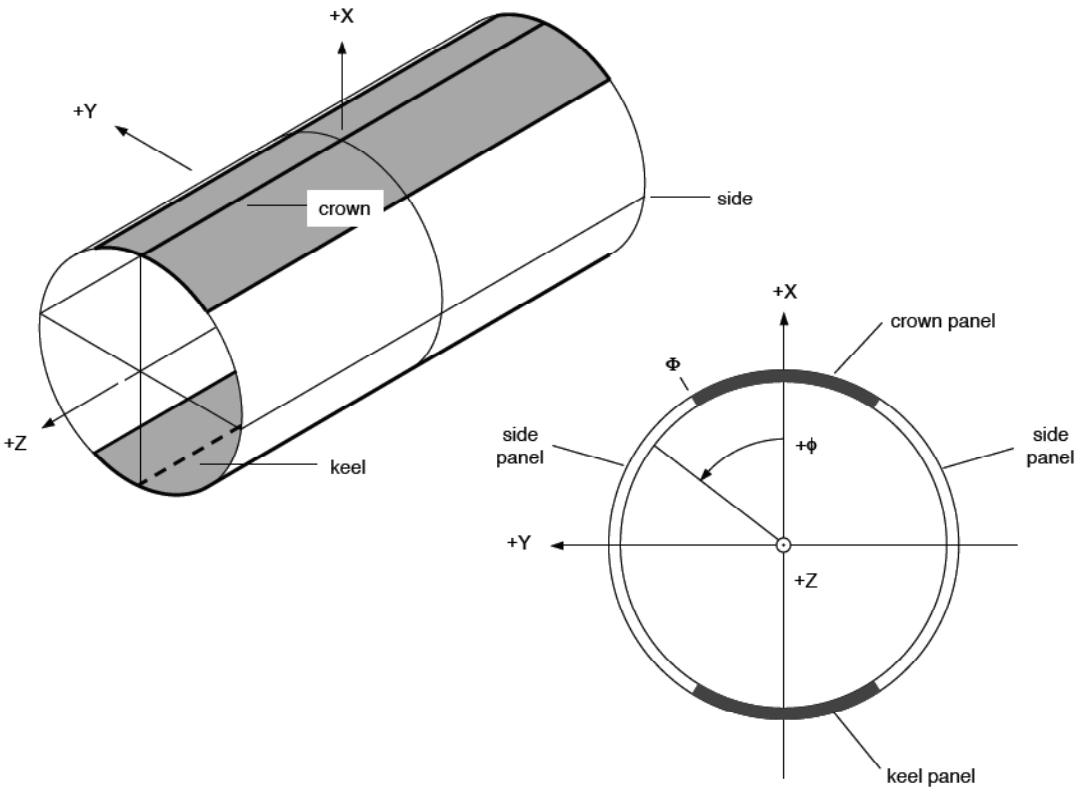

Figure 12a. Shell with crown/keel panels schematic.

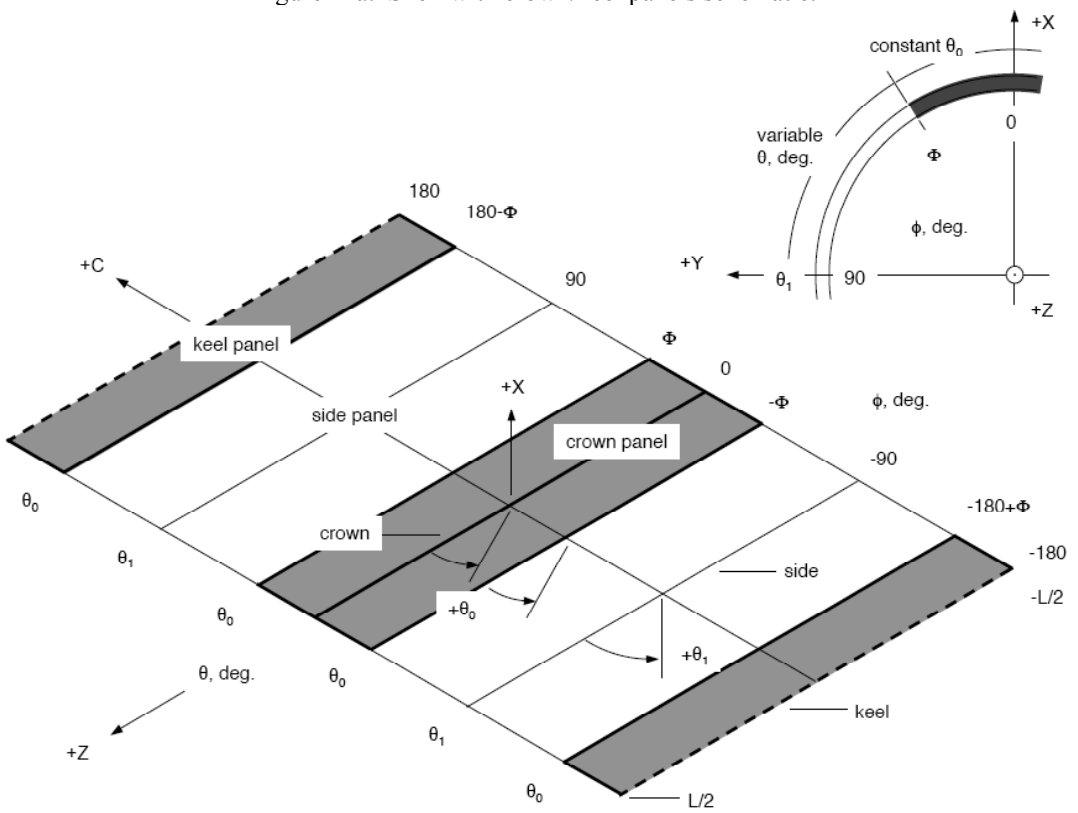

Figure 12b. Shell with crown/keel panels planform.

isotropic shell. To improve the structural performance of the tow-steered shell, the 8-ply design without overlaps is modified to incorporate crown/keel and side panels (shown in Figure 12) having different fiber orientation angles. The crown/keel panels each cover 2Φ degrees of arc, and contain fibers with a constant orientation angle θ_0. The side panels each cover $(180\text{-}2\Phi)$ degrees of arc, and are symmetric about the shell sides. The crown and side panels intersect at an angle of Φ degrees.

The fiber orientation angle ranges from θ_0 at the intersection with the crown/keel panels, to θ_1 at the shell side, and back to θ_0. Note that the crown/keel panels degenerate to lines for a shell with $\Phi = 0$ degrees, which is the design evaluated in the previous sections. A configuration with $\Phi = 90$ degrees has all four tow-steered plies replaced with straight-fiber plies with $\theta = \pm\theta_0$. A representative tow-steered ply with $\Phi = 30$, $\theta_0 = 0$, and $\theta_1 = 45$ degrees is shown in Figure 13.

Classical methods developed from strength of materials theory are used to predict the static bending stiffnesses for tow-steered shells without overlaps over wide ranges of Φ and θ_0. These stiffnesses are then compared with corresponding values for a quasi-isotropic shell. The axial elastic modulus $E_Z(\theta)$ of an 8-ply $[\pm45/\pm\theta]_S$ laminate (with θ varying from 0 to 45 degrees) is first computed using classical lamination theory and the listed material properties.

The axial stiffness of a shell wall increment (see Figure 1a) is calculated by multiplying the appropriate elastic modulus $E_Z(\theta)$ by the differential area $dA = (R \times d\phi \times t)$. The parallel axis theorem is then used to compute the shell principal bending stiffnesses, where the shell wall axial stiffness increments and the squares of the distances of the differential areas from the X- or Y-axes are summed around the entire shell circumference. An arc length $d\phi$ of 1 degree is used here.

Bending stiffnesses are calculated using these methods for values of Φ from 0 to 90 degrees, and θ_0 from 0 to 15 degrees, both in 5-degree increments. The principal bending stiffnesses for these modified tow-steered shells are plotted in Figure 14, and increase rapidly with increasing values of Φ. This is due in large part to the increased bending stiffness of the expanded crown/keel panels, which greatly improves that measure of the shell structural performance.

Bending stiffnesses of the tow-steered shell without overlaps (see Figure 9) are shown as solid circles in Figure 14. The predicted bending stiffnesses for that configuration (listed in Table II) compare very well with corresponding results from the finite element analyses, with an average difference of less than 1 percent. The open circles in Figure 14 denote the principal bending stiffnesses for the crown/keel panel shell configuration shown in Figure 13, which are much higher than for the shell without overlaps. About 10 percent of the performance increase is due to the 0-degree fiber orientation angle, with about 20 percent from the crown/keel panels.

The calculated bending stiffness of the quasi-isotropic shell is also shown in Table II and plotted in Figure 14. This stiffness is the product of the quasi-isotropic layup axial modulus $E_Z = 7.332$ Mlb/in^2 and the approximate shell moment of inertia ($\pi \times R^3 \times t = 118.075$ in^4). The calculated and computed bending stiffnesses of the quasi-isotropic shell are also very close, with a 0.2 percent difference between them.

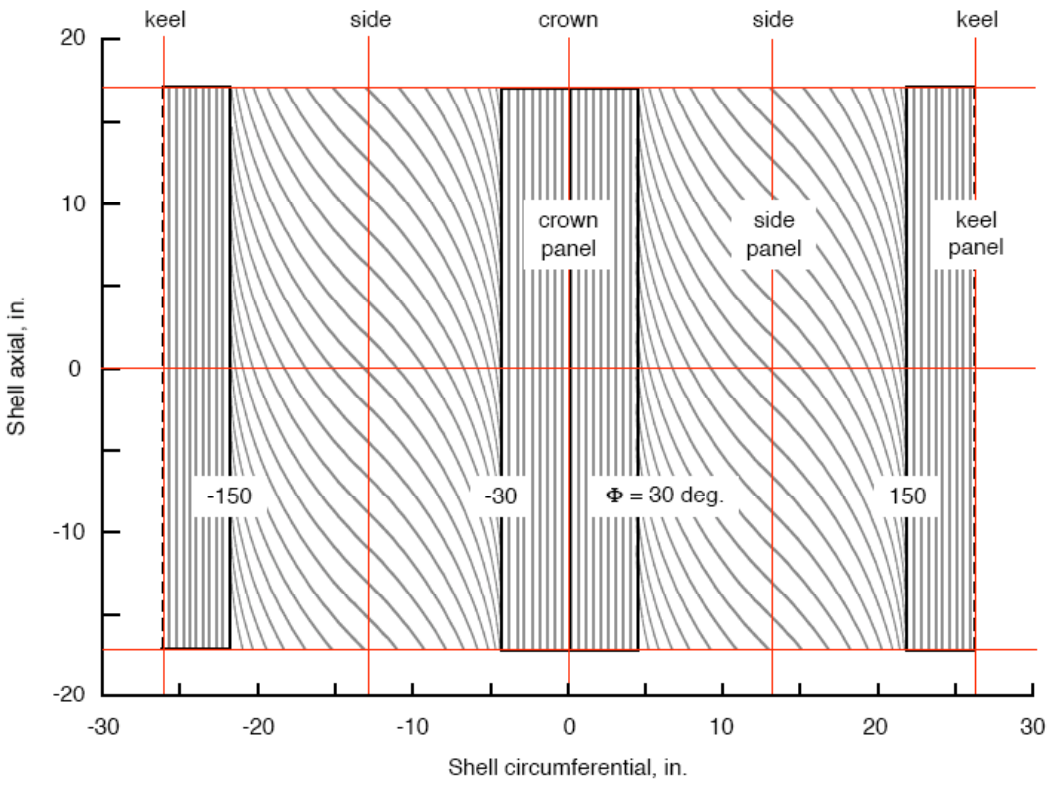

Figure 13. Tow paths for representative shell with crown/keel panels.

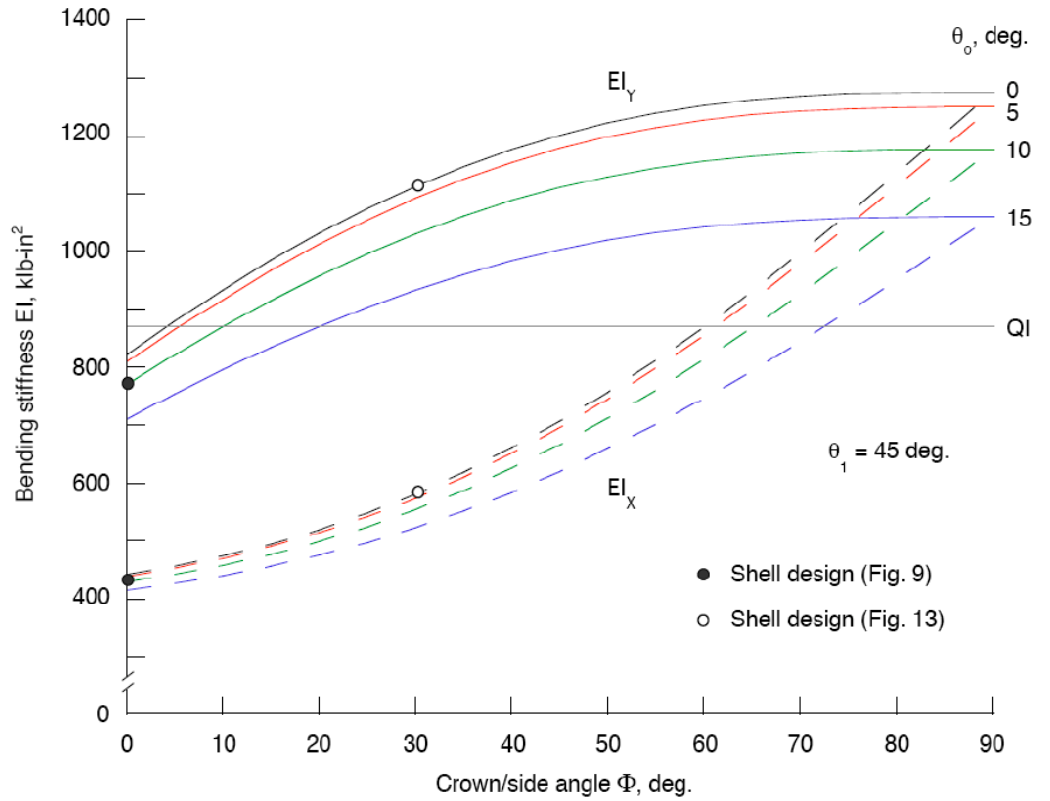

Figure 14. Bending stiffnesses of shells with crown/keel panels.

Figure 14 shows that large increases in the Y-axis shell bending stiffnesses are possible by increasing the shell crown/side angle, and that the quasi-isotropic shell bending stiffness can be matched using relatively small values of Φ up to 20 degrees. Much larger values of Φ (as high as 70 degrees) are required for the X-axis shell bending stiffnesses to equal the quasi-isotropic shell bending stiffness. Small reductions in the bending stiffnesses are noted when θ_0 is varied from 0 to 5 degrees, which may be desirable to avoid having large numbers of adjacent 0-degree plies. The reductions in bending stiffnesses increase more rapidly for the larger values of θ_0.

CONCLUDING REMARKS

In this study, the structural performance of a proposed tow-steered shell design is evaluated using finite element analyses and classical methods. This design is intended to represent the fuselage of an advanced aircraft subjected to bending moments. As the composite tows are placed on a cylindrical mandrel, they are steered along circular arcs using a computer-controlled fiber placement machine. This allows the fibers to be better aligned with the load paths, which put the upper and lower surfaces of the fuselage into compression and tension (respectively), and the fuselage sides into shear.

Two shells with the same fiber patterns are analyzed, one with tow overlaps, and one without. Both shells have a fiber orientation angle that varies continuously from 10 degrees on the crown and keel lines to 45 degrees on the sides. The shell with tow overlaps shows improved buckling load and stiffness for Y-axis bending when compared to a quasi-isotropic shell. To further improve the shell structural performance, an angle-ply crown/keel panel is incorporated into the design, and the bending stiffnesses of this configuration are evaluated using classical methods. Large increases in the shell bending stiffnesses are also possible for this configuration. However, further work is still required to refine this concept and incorporate the many practical details needed for an actual flight vehicle structure.

REFERENCES

1. Evans, D. O., M. M. Vaniglia, and P. C. Hopkins. 1989. "Fiber Placement Process Study," presented at the 34th International SAMPE Symposium, May 8-11, 1989.
2. Wu, K. C., and Z. Gürdal. 2001. "Thermal Testing of Tow-Placed, Variable Stiffness Panels," presented at the 42nd AIAA/ASME/ASCE/AHS/ASC Structures, Structural Dynamics and Materials Conference, April 16-19, 2001.
3. Alhajahmad, A., M. M. Abdalla, and Z. Gürdal. 2008. "Design Tailoring for Pressure Pillowing Using Tow-Placed Steered Fibers," *Journal of Aircraft*, 45(2): 630-640.
4. Jegley, D. C., B. F. Tatting, and Z. Gürdal. 2005. "Tow-Steered Panels with Holes Subjected to Compression or Shear Loading," presented at the 46th AIAA/ASME/ASCE/AHS/ASC Structures, Structural Dynamics and Materials Conference, April 18-21, 2005.
5. Tatting, B. F., and Z. Gürdal. 1998. "Design and Manufacture of Tow-Placed Variable Stiffness Composite Laminates with Manufacturing Considerations," presented at the 13th U.S. National Congress of Applied Mechanics, June 21-26, 1998.

6. Rankin, C. C., F. A. Brogan, W. A. Loden, and H. D. Cabiness. January 2005. "STAGS User Manual, Version 5.0," Lockheed Martin Missiles & Space Co., Inc., Palo Alto, California.
7. Beer, F. P., and E. R. Johnson, Jr. 1981. *Mechanics of Materials*. McGraw-Hill, Inc., pg. 598.

TABLE I. NUMBER OF COURSES REQUIRED AS A FUNCTION OF THE NUMBER OF TOWS PLACED PER COURSE AND STEP-OVER

Number of tows placed per course	Number of courses with step-over ε =								
	0 in.	0.005	0.010	0.015	**0.020**	**0.025**	0.030	0.035	0.040
6	24.182	24.022	23.864	23.708	23.554	23.402	23.252	23.104	22.958
7	20.728	20.610	20.493	20.378	20.264	20.152	20.040	19.930	19.821
8	18.137	18.046	17.957	17.869	17.781	17.694	17.608	17.523	17.439
9	16.121	16.050	15.979	15.909	15.840	15.771	15.703	15.635	15.568
10	14.509	14.451	14.394	14.337	14.281	14.225	14.169	14.114	14.059
11	13.190	13.142	13.095	13.048	13.001	12.955	12.909	12.863	12.817
12	12.091	12.051	12.011	11.971	11.932	11.893	11.854	11.815	11.777
13	11.161	11.127	11.093	11.059	11.025	10.992	10.959	10.926	10.893
14	10.364	10.334	10.305	10.276	10.247	10.218	10.189	10.161	10.132
15	9.673	9.647	9.622	9.596	9.571	9.546	9.521	9.496	9.471
16	9.068	9.046	9.023	9.001	8.979	8.956	8.934	8.912	8.890
17	8.535	8.515	8.495	8.475	8.455	8.436	8.416	8.397	8.377
18	8.061	8.043	8.025	8.007	7.990	7.972	7.955	7.937	7.920
19	7.636	7.620	7.604	7.589	7.573	7.557	7.541	7.526	7.510
20	7.255	7.240	7.226	7.211	7.197	7.183	7.169	7.154	7.140
21	6.909	6.896	6.883	6.870	6.857	6.844	6.831	6.818	6.805
22	6.595	6.583	6.571	6.559	6.548	6.536	6.524	6.512	6.501
23	6.308	6.297	6.287	6.276	6.265	6.254	6.243	6.233	6.222
24	6.046	6.035	6.025	6.015	**6.005**	**5.996**	5.986	5.976	5.966

TABLE II. TOW-STEERED AND QUASI-ISOTROPIC SHELL STRUCTURAL PERFORMANCE

	Shell with overlaps	Shell without overlaps	Quasi-isotropic shell
FE bending EI_X, Mlb-in^2	522.336	438.823	868.074
Buckling for X-axis moment, klb-in.	367.223	287.245	428.335
FE bending EI_Y, Mlb-in^2	1465.803	780.882	868.074
Buckling for Y-axis moment, klb-in.	589.271	210.207	428.335
SM bending EI_X, Mlb-in^2	–	429.437	871.384
SM bending EI_Y, Mlb-in^2	–	771.175	871.384